Critical conditions for development of a second pair of Dean vortices in curved microfluidic channels

Minyoung Kim and Ali Borhan*

Department of Chemical Engineering, The Pennsylvania State University, University Park, Pennsylvania 16802, USA

(Received 6 January 2023; accepted 20 April 2023; published 11 May 2023)

The centrifugal force in flow through a curved channel initiates a hydrodynamic instability that results in the development of Dean vortices, a pair of counter-rotating roll cells across the channel that deflect the high velocity fluid in the center toward the outer (concave) wall. When this secondary flow toward the concave (outer) wall is too strong to be dissipated by viscous effects, an additional pair of vortices emerges near the outer wall. Combining numerical simulation and dimensional analysis, we find that the critical condition for the onset of the second vortex pair depends on $\gamma^{1/2}\mathrm{Dn}$ (γ: channel aspect ratio; Dn: Dean number). We also investigate the development length for the additional vortex pair in channels with different aspect ratios and curvatures. The larger centrifugal force at higher Dean numbers produces the additional vortices further upstream, with the required development length being inversely proportional to the Reynolds number and increasing linearly with the radius of curvature of the channel.

DOI: 10.1103/PhysRevE.107.055103

I. INTRODUCTION

Fluid flow in curved channels has been widely studied because of its ubiquitous nature in both natural and industrial settings such as meandering rivers and heat exchangers. The original work of Dean showed that the centrifugal forces generated by channel curvature initiate a hydrodynamic instability that leads to the development of a pair of counter-rotating vortices that deflect the high velocity fluid in the center toward the outer (concave) wall of the channel [1]. Since then, numerous studies of the applications of Dean flow have shown that the secondary flow resulting from the centrifugal instability can enhance mixing and heat and mass transfer. An important consideration in these applications is the formation of an additional pair of vortices near the outer (concave) wall of the curved channel. Near the center of the channel cross section, the secondary flow is directed toward the outer wall where it is dissipated by viscous effects. When the secondary flow is too strong to be dissipated, however, an additional vortex pair appears.

The existence of the additional vortex pair was first mentioned by Cheng and Akiyama [2]. While computing the secondary flow structure in a curved rectangular channel, they found the additional vortices above a critical Dean number. The presence of the additional vortex pair was later confirmed by both numerical simulations and experimental observations. Ghia and Sokhey [3] and Soh [4] presented computational results for the development of the second pair of vortices in curved channels with square and rectangular cross sections, while Sugiyama *et al.* [5] and Bara *et al.* [6] performed direct visualization of the additional vortices in their experiments. Using bifurcation analysis, Winters [7], Rigo *et al.* [8], and Haines *et al.* [9] also found the existence of multiple solutions for fully developed flow in square and high-aspect-ratio rectangular channels. Most recently, Nivedita *et al.* [10] tried to take advantage of the development of multiple vortices for particle focusing, but the flow structure they observed via direct visualization was different from that predicted by previous computational studies in that the additional vortices were not located near the outer wall and rotated in the opposite direction. Sivasankar *et al.* [11] and Do *et al.* [12] reported that the presence of particles in flow through curved channels alters the secondary flow structure [11,12] and the number of vortices [11]. These observations underscore the need for a better understanding of the formation of additional vortices.

While previous studies have established the formation of a second pair of vortices, the critical conditions for the onset of the additional vortex pair have not been well characterized. For flows in curved channels of rectangular cross section, the critical condition for the formation of the second pair of vortices depends on the channel aspect ratio [5,9]. Moreover, for fixed aspect ratio, the channel length required for development of the additional vortex pair must be established to guide practical applications. The purpose of this study is to establish the critical conditions for the formation of a second pair of Dean vortices in rectangular channels of different aspect ratio. We also examine the development length for the formation of the additional vortex pair and show that a greater centrifugal force at higher Dean numbers accelerates the onset of secondary flow and moves the first appearance of a second vortex pair upstream.

II. METHODS

The flow configuration for the computational fluid dynamics analysis consists of a curved channel with centerline radius of curvature R and rectangular cross section of width

*borhan@psu.edu

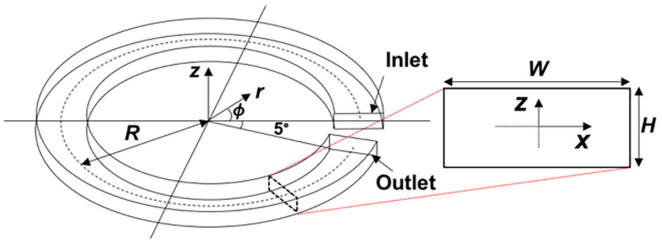

FIG. 1. Computational domain for a curved channel with centerline radius of curvature R, width W in the radial (r) direction, and height H in the axial (z) direction.

W and height H (Fig. 1). The flow domains were created and meshed using hexahedral elements in ICEM-CFD (Ansys, Inc., Canonsburg, PA) and imported to FLUENT (Ansys, Inc., Canonsburg, PA). A pressure-based finite volume method was used to solve the steady-state continuity and Navier-Stokes equations subject to uniform velocity U_0 at the inlet, no-slip on the walls, and zero viscous normal stress at the outlet. Mesh refinement was performed until the converged solutions were insensitive to further reduction in mesh size (see Appendix A for details). The cross-sectional area of the channel (HW) was fixed and the geometrical parameters R, W, and H, as well as the flow rate, were varied to probe the flow structure over a wide range of the dimensionless parameters listed in Table I; namely, the aspect ratio of the channel cross section $\gamma \equiv H/W$, dimensionless curvature $\alpha \equiv D_h/2R$, Reynolds number $\mathrm{Re} \equiv \rho U_0 D_h/\mu$, and Dean number $\mathrm{Dn} \equiv \alpha^{1/2}\mathrm{Re}$, where ρ and μ are the fluid density and viscosity, respectively, $D_h = 2H/(1+\gamma)$ is the hydraulic diameter of the channel, and U_0 is the average velocity through the channel. Channels with aspect ratios in the range $0.15 \leqslant \gamma \leqslant 1.0$ and dimensionless centerline curvatures ranging from 0.014 to 0.089 were used in the computations.

III. RESULTS AND DISCUSSION

The primary and secondary flow patterns over the cross section located 7/8 of a revolution from the channel inlet (i.e., at $\phi = 7\pi/4$) are shown in Fig. 2 for channel C2 of Table I characterized by $\gamma = 0.20$ and $\alpha = 0.022$, where the transition to two vortex pairs occurs when $\gamma^{1/2}\mathrm{Dn} \simeq 110$. This is in good agreement with the observed conditions for the formation of the second vortex pair in previous experimental studies. The reported values of $\gamma^{1/2}\mathrm{Dn}$ for the experimentally observed transition are in the range of 97 to 119 for channels with aspect ratios in the range $0.5 \leqslant \gamma \leqslant 1$ [5,6].

TABLE I. Channel dimensions and dimensionless parameters used in the computations.

Channel no.	R (mm)	H (mm)	γ	α	Max Re	Max Dn
C1	15.0	0.69	0.15	0.040	1630	327
C2	30.0	0.80	0.20	0.022	1940	290
C3	10.0	0.98	0.30	0.075	1410	388
C4	40.0	0.98	0.30	0.038	1880	259
C5	60.0	1.13	0.40	0.014	1940	224
C6	20.0	1.27	0.50	0.042	1410	289
C7	30.0	1.39	0.60	0.029	1800	306
C8	10.0	1.60	0.80	0.089	1110	331
C9	60.0	1.79	1.0	0.014	1490	182

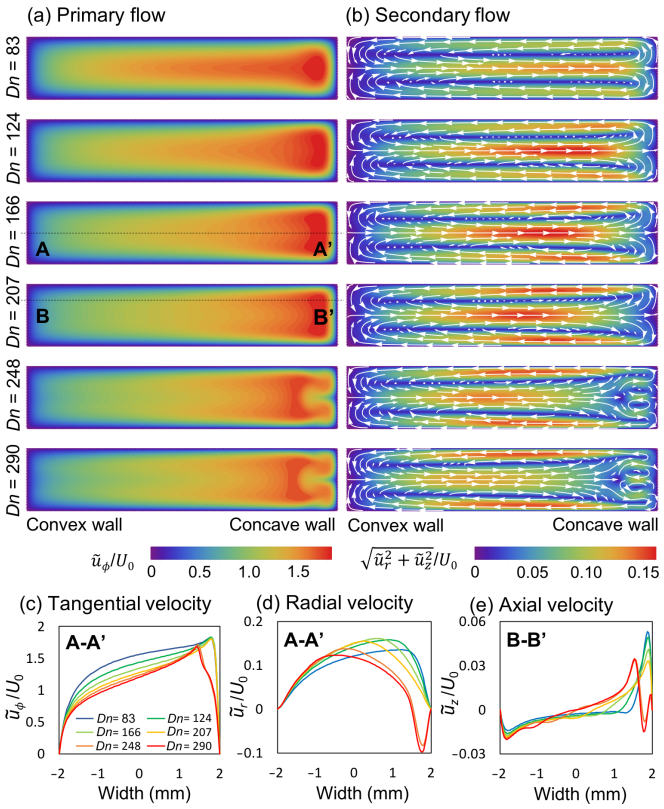

FIG. 2. (a) Primary flow and (b) secondary flow structures at 7/8 revolution from the inlet of the curved channel with $\gamma = 0.20$ and $\alpha = 0.022$. An additional vortex pair is formed near the concave wall for $\mathrm{Dn} = 248$ and $\mathrm{Dn} = 290$. (c) Tangential velocity and (d) radial velocity profiles along the centerline (A-A′) and (e) axial velocity profile at distance $H/4$ from the top wall (B-B′).

To gain more insight, we consider the dimensionless radial momentum equation,

$$u_r\frac{\partial u_r}{\partial r} + u_z\frac{\partial u_r}{\partial z} - \frac{u_\phi^2}{r} = -\frac{\partial p}{\partial r} + \frac{1}{\gamma^{1/2}\mathrm{Dn}_H}\left[\frac{\partial^2 u_r}{\partial z^2} + \gamma^2\frac{\partial^2 u_r}{\partial r^2} + \alpha\gamma(1+\gamma)\frac{1}{r}\frac{\partial u_r}{\partial z} - \alpha^2(1+\gamma)^2\frac{u_r}{r^2}\right], \quad (1)$$

where r is made dimensionless with R, the variations in the r and z directions occur over length scales W and H, respectively, the tangential velocity is scaled with U_0, the radial velocity with $(W/R)^{1/2}U_0$, the axial velocity with $\gamma(W/R)^{1/2}U_0$, and the pressure with $\rho(W/R)U_0^2$. The characteristic radial velocity $(W/R)^{1/2}U_0$ is established by a balance between convective acceleration and centrifugal force within the channel cross section. The parameter $\mathrm{Dn}_H = (1+\gamma)^{3/2}\mathrm{Dn}$ denotes the Dean number based on the characteristic length $\lim_{\gamma\to 0} D_h = 2H$, i.e., the Dean number for very low-aspect-ratio channels. Since the radius of curvature of the channel centerline is typically much larger than the

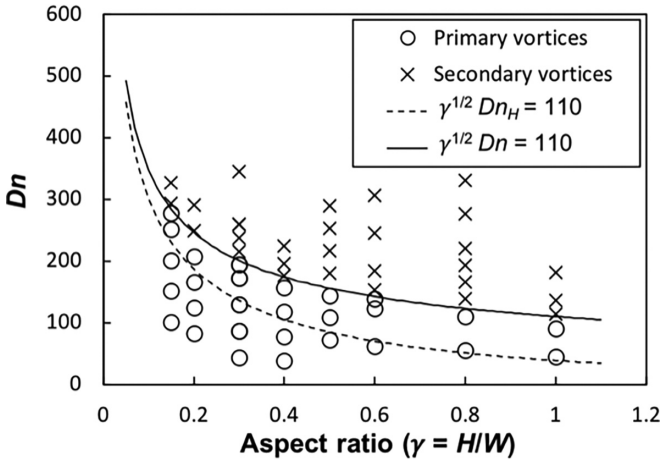

FIG. 3. Critical conditions for development of secondary Dean vortices.

channel's hydraulic diameter ($\alpha \ll 1$), the last two terms on the right-hand side of Eq. (1) are negligible. For low-aspect-ratio channels, the first viscous term on the right-handside of Eq. (1) can stabilize the flow when the parameter $\gamma^{1/2}\mathrm{Dn}_H$ is smaller than a critical value (found to be ~110), resulting in a single pair of counter-rotating vortices [see the secondary flow structure for $\mathrm{Dn} \leqslant 207$ in Fig. 2(b)]. When $\gamma^{1/2}\mathrm{Dn}_H$ exceeds the critical value, viscous effects are too weak to dissipate convective acceleration and an additional pair of vortices appears [see the secondary flow structure for $\mathrm{Dn} \geqslant 248$ in Fig. 2(b)]. The detailed velocity profiles described in Figs. 2(c)–2(e) show qualitatively different behavior near the outer wall depending on the presence of the additional vortices. They suggest that inspection of the sign of the midplane radial velocity [presented in Fig. 2(d)] can be used to detect the presence of the second vortex pair.

As the channel aspect ratio increases, the critical value of $\gamma^{1/2}\mathrm{Dn}_H$ for the first appearance of the second vortex pair becomes larger. This may be attributed to the additional stabilizing contribution from the second viscous term on the right-hand side of Eq. (1), which is no longer negligible as $\gamma \to 1$. Our computational results show that the critical value of $\gamma^{1/2}\mathrm{Dn}_H$ grows like $(1+\gamma)^{3/2}$ as $\gamma \to 1$, and the critical condition can be conveniently written as $\gamma^{1/2}\mathrm{Dn} = 110$, represented by the solid curve in Fig. 3, which asymptotically approaches the dotted curve $\gamma^{1/2}\mathrm{Dn}_H = 110$ as $\gamma \to 0$. Hence, using a Dean number based on hydraulic diameter, the critical value of $\gamma^{1/2}\mathrm{Dn}$ is independent of the channel aspect ratio.

For channels with large aspect ratio ($\gamma \gg 1$), the viscous effect is dominated by the second term in the square brackets on the right-hand side of Eq. (1), which is $\mathcal{O}(\mu U_C/W^2)$. Hence, the dimensionless parameter that determines the formation of the second pair of vortices is expected to be $\mathrm{Dn}_H/\gamma^{3/2} = \mathrm{Dn}_W$, where Dn_W is the Dean number based on the characteristic length $\lim_{\gamma\to\infty} D_h = 2W$ and Dn approaches Dn_W as $\gamma \to \infty$. This is consistent with the bifurcation analysis of Haines *et al.* [9] for high-aspect-ratio channels, which showed that the critical condition for secondary flow transition from one pair of vortices to multiple vortices is $\mathrm{Dn}_W \simeq 100$ for $\gamma \geqslant 7$ [13].

For channels with small aspect ratio ($\gamma \ll 1$), on the other hand, the viscous effect is dominated by the first term in the square brackets on the right-hand side of Eq. (1), which is $\mathcal{O}(\mu U_C/H^2)$. The viscous friction at the top and bottom channel walls and momentum transfer to the walls from the center of the channel dissipates the secondary flow directed toward the outer wall and delays the formation of the second vortex pair. Therefore, a stronger secondary flow (higher Dn_H or Dn) is required for the formation of the additional vortices as $\gamma \to 0$ and the flow transition depends on the dimensionless parameter $\gamma^{1/2}\mathrm{Dn}_H$ or $\gamma^{1/2}\mathrm{Dn}$, as suggested by dimensional analysis [Eq. (1)] and simulations (Fig. 3).

In addition to the critical value of the Dean number that must be exceeded for the formation of the second vortex pair, we investigate the channel length required for development of the additional vortices. Figure 4(a) shows the development of secondary flow in a curved channel with $\gamma = 0.60$ and $\alpha = 0.029$ (Channel C7 in Table I) at $\mathrm{Dn} = 153$. At 1/2 revolution from the inlet (i.e., at $\phi = \pi$), the secondary vortices emerge near the outer wall and continue to develop until $\phi = 3\pi/2$. As described earlier, the sign of the midplane radial velocity near the outer wall can serve as a marker for determining whether secondary flow has a two-cell or four-cell pattern. Moreover, in simulations with channel aspect ratios of $0.15 \leqslant$

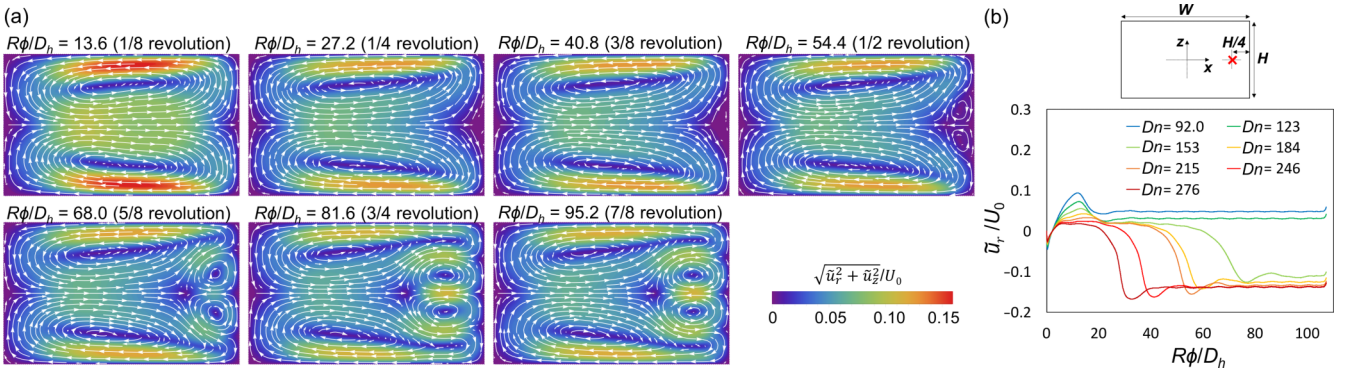

FIG. 4. Flow development for a uniform inlet-velocity profile in a channel with $\gamma = 0.60$ and $\alpha = 0.029$ (Channel C7 in Table I) at $\mathrm{Dn} = 153$. (a) Secondary flow structure at different channel cross sections, and (b) normalized radial velocity ($\tilde{u}_r/|U_0|$) at a point on the centerline of the channel cross section a distance $H/4$ from the outer wall (indicated by the red X). Secondary vortices emerge after the 1/2 revolution and develop until the 3/4 revolution.

$\gamma \leqslant 1.0$, the size of the additional vortex was of the order of a quarter of the channel height [$H/4$; see Figs. 2(b) and 4(a) for $\gamma = 0.20$ and 0.60, respectively]. Hence, the sign of the radial velocity at the point $(x, z) = (W/2 - H/4, 0)$ was used to detect the formation of the additional vortex pair. The development of the radial velocity with distance from the channel inlet is shown in Fig. 4(b) for the point $(x, z) = (W/2 - H/4, 0)$, indicated by the red X mark near the outer wall. The centrifugal force generated by channel curvature accelerates the lateral flow across the channel cross section to develop the secondary flow. Near the inlet, only one pair of counter-rotating vortices appears because the secondary flow is not strong enough to create an additional pair of vortices. When the secondary flow toward the concave (outer) wall becomes accelerated downstream and too strong to be dissipated by viscous effects, the second pair of vortices emerges near the outer wall. As the Dean number increases, the stronger centrifugal acceleration creates the additional vortices further upstream in the channel, as shown in Fig. 4(b). Whereas the development length of two-cell flow increases with Reynolds number [14,15], the development length of four-cell flow decreases with increasing Dean number. This is consistent with previous numerical results for flow within a curved square channel ($\gamma = 1$) with fixed channel curvature [6].

The flow structure reported by Nivedita *et al.* [10], wherein the second pair of vortices rotates in the same direction as the first pair of Dean vortices (i.e., counterclockwise in the upper half of the channel), was not found in our simulations with a uniform inlet velocity. However, a flow structure resembling that reported by Nivedita *et al.* [10] was observed for developing flow with a parabolic inlet-velocity profile [at $R\phi/D_h = 13.6$ in Fig. 7(a) in Appendix B]. The observed flow structure was transient in nature and the fully developed secondary flow structure was the same as that obtained for a uniform inlet-velocity profile (i.e., with the additional pair of vortices rotating clockwise in the upper half of the channel). The parabolic inlet-velocity profile required a shorter channel length for development of the second vortex pair [Fig. 4(b) and Fig. 7(a) in Appendix B].

Based on the results for secondary flow development from a uniform inlet-velocity profile (Fig. 4), we define a development length for the second vortex pair as the distance L from the channel inlet to the channel cross section in which the midplane ($z = 0$) radial velocity at a distance $H/4$ from the outer wall [point X in Fig. 4(b)] achieves a minimum. The computed development lengths for different flow rates in the microchannels of Table I are shown in Fig. 5. Least-squares regression of the results in this figure (with $R^2 = 0.96$) indicates that for a fixed microchannel, the required channel length for the development of two pairs of Dean vortices is inversely proportional to the Dean number. More specifically,

$$\frac{L}{2H} = k_1(\alpha^{1/2}\gamma^{1/2}\mathrm{Dn}_H)^{-k_2} \tag{2}$$

or, equivalently,

$$\frac{L}{D_h} = k_1(1+\gamma)^{1-3k_2/2}(\alpha^{1/2}\gamma^{1/2}\mathrm{Dn})^{-k_2}, \tag{3}$$

where $k_1 = 1470$ and $k_2 = 0.978$. This represents a characterization of the development length for different channel aspect ratios. According to these results, the development length increases linearly with the radius of curvature of the microchannel so that the azimuthal angle at development length, ϕ_L, is independent of the radius of the curvature; namely,

$$\phi_L \equiv \frac{L}{R} \simeq \frac{2k_1}{[\gamma(1+\gamma)]^{1/2}\mathrm{Re}}. \tag{4}$$

Hence, in a helical microchannel, the number of revolutions required for development of the second pair of Dean vortices is expected to be inversely proportional to the flow Reynolds number. Noting that the critical condition for the formation of the second vortex pair requires $\mathrm{Re} > 110(\alpha\gamma)^{-1/2}$, the additional vortex pair is always expected to develop in less than one revolution for laminar flow with $\gamma^{1/2}\mathrm{Dn} > 110$ in channels with $\alpha < 0.055(1+\gamma)$. The latter condition was satisfied by all microchannels in Table I, except C3. For channels with $\alpha > 0.055(1+\gamma)$, development of the additional vortex pair in less than one channel revolution can be achieved only when $\mathrm{Re} > 470[\gamma(1+\gamma)]^{-1/2}$.

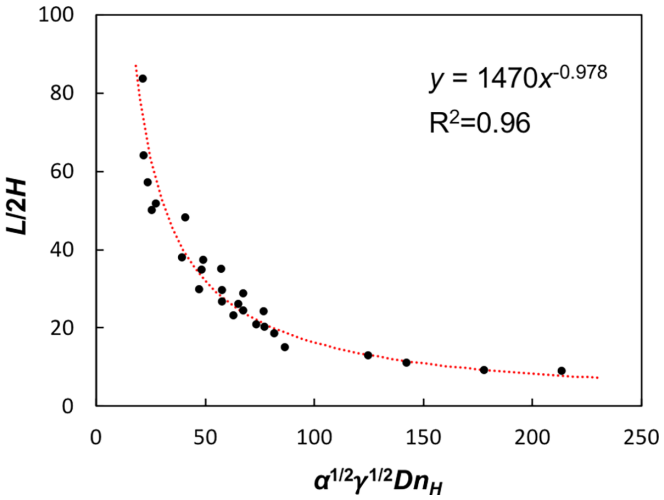

FIG. 5. Dimensionless channel length $L/2H$ required for development of the second vortex pair.

IV. CONCLUSIONS

Computations of steady flow in curved microfluidic channels of different aspect ratio reveal the conditions for the onset of secondary Dean vortices. Depending on the magnitude of the parameter $\gamma^{1/2}\mathrm{Dn}$, different secondary flow structures

TABLE II. Mesh characteristics for the mesh refinement study.

Mesh	No. elements across channel height	No. elements across channel width	Element size (mm)	Total no. elements
M1	20	40	0.063	2.6×10^6
M2	32	64	0.040	6.4×10^6
M3	40	80	0.032	9.8×10^6
M4	52	104	0.024	1.63×10^7
M5	60	120	0.021	2.15×10^7
M6	72	144	0.018	2.40×10^7

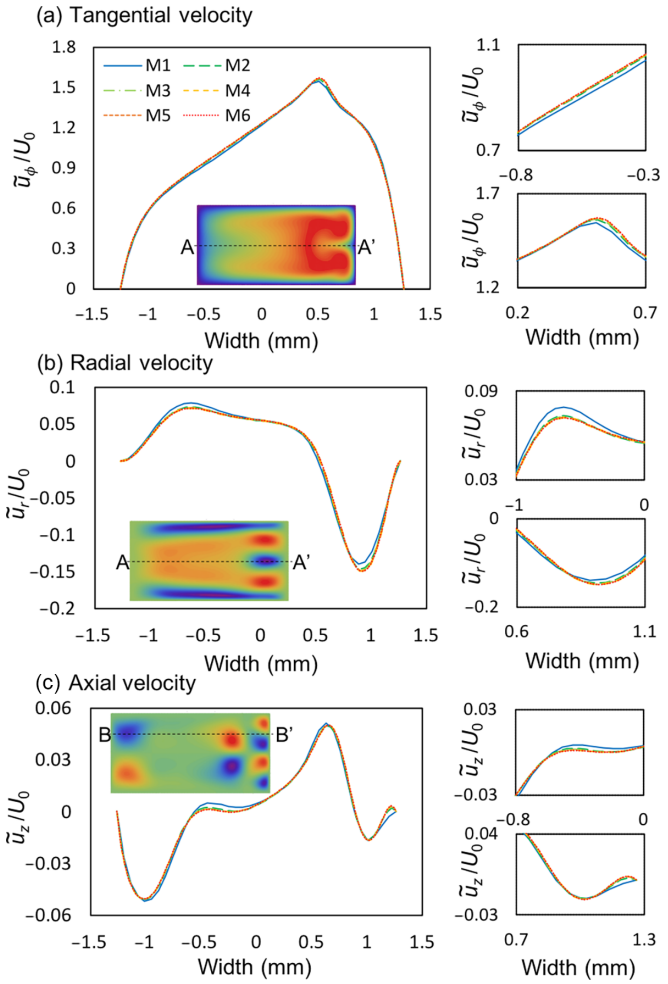

FIG. 6. Computed velocity profiles for mesh structures M1–M6 of Table II. (a) Tangential velocity and (b) radial velocity profiles along A-A′ at the centerline of the channel cross section, and (c) axial velocity profile along B-B′ at distance $H/4$ from the top wall. The images on the right side represent magnified views of the velocity profiles.

can be generated. In particular, as $\gamma^{1/2}\mathrm{Dn}$ exceeds 110, the secondary flow structure transitions from one pair of counter-rotating vortices to two pairs of vortices, with the new vortex pair developing near the outer (concave) wall. The transition Dean number for the formation of the second pair of vortices decreases with increasing channel aspect ratio. The channel length required for the development of the additional vortex pair decreases inversely with the Reynolds number and is linearly proportional to the radius of curvature of the channel. The results of this study can be used to guide channel design for active modulation of the critical condition and development length for the formation of secondary Dean vortices, which can significantly affect performance in applications such as vortex-induced reaction [16] and particle capture and separation [17] in curved microchannels.

APPENDIX A: MESH REFINEMENT

The curved channel geometries were created and meshed with hexahedral elements using ICEM-CFD (Ansys, Inc., Canonsburg, PA). The meshed geometries were then imported into FLUENT (Ansys, Inc., Canonsburg, PA) to solve the mass and momentum conservation equations using a pressure-based finite volume method. The solution was considered to be converged when the residuals remained less than 10^{-5}. The mesh was refined, as shown in Table II, until converged solutions became insensitive to further mesh refinement. About 3000 elements were used along the length of the channel for all six different grid structures M1–M6 in the mesh refinement study. Doubling the number of elements along the length of the channel did not have a significant effect on the results. The results of a typical mesh refinement study are shown in Fig. 6 for channel C6 of Table I (with centerline curvature $R = 20.0$ mm, width $W = 2.53$ mm, and height $H = 1.27$ mm). In this case, mesh refinement from M5 to M6 resulted in less than a 0.1% change in the computed velocity profiles and thus mesh structure M5 was sufficient to accurately capture the flow field.

APPENDIX B: FLOW DEVELOPMENT WITH A PARABOLIC INLET-VELOCITY PROFILE

To examine the effect of the inlet-velocity profile on secondary flow development, we performed the computations

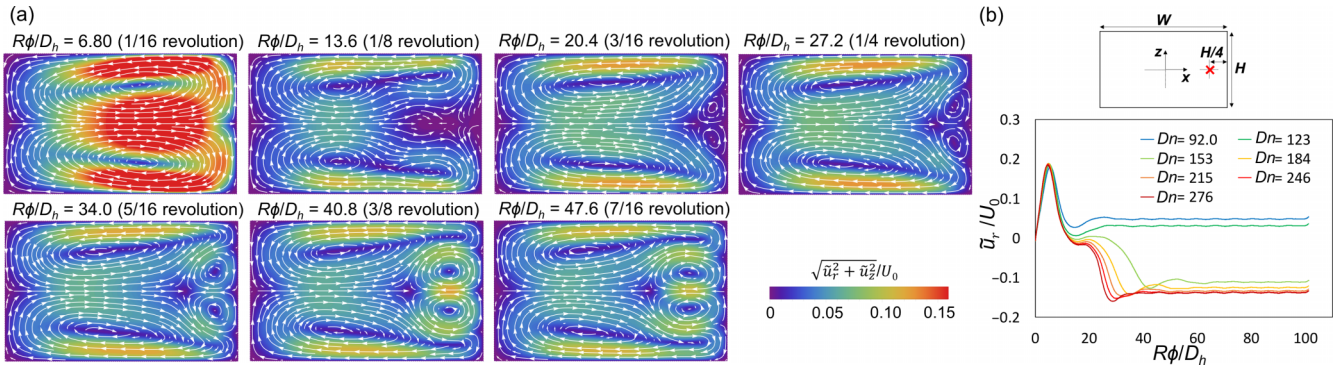

FIG. 7. Flow development for a parabolic inlet-velocity profile in a channel with $\gamma = 0.60$ and $\alpha = 0.029$ (Channel C7 in Table I) at $\mathrm{Dn} = 153$. (a) Secondary flow structure at different channel cross sections. Secondary vortices emerge after the 3/16 revolution and develop until the 7/16 revolution, and (b) normalized radial velocity ($\tilde{u}_r/|U_0|$) at a point on the centerline of the channel cross section a distance $H/4$ from the outer wall.

with a parabolic velocity profile at the inlet. Figure 7(a) shows the development of the normalized radial velocity ($\tilde{u}_r/|U_0|$) in channel C7 of Table I (with aspect ratio 0.60) at the same location on the channel cross section as that defined in Fig. 4. Comparison with the corresponding results shown in Fig. 4 for a uniform inlet-velocity profile shows that although the parabolic inlet-velocity profile leads to an earlier appearance of the secondary Dean vortices, it produces the same final flow structure (as that for uniform inlet velocity) at the same flow rate. It is worth noting that the secondary flow structure after 1/8 revolution (Fig. 7) is qualitatively similar to that reported by Nivedita *et al.* [10], wherein the additional vortices appear to rotate in the opposite direction compared to those reported from other experiments [5,6].

[1] W. R. Dean, Fluid motion in a curved channel, Proc. R. Soc. London A **121**, 402 (1928).

[2] K. C. Cheng and M. Akiyama, Laminar forced convection heat transfer in curved rectangular channels, Intl. J. Heat Mass Transf. **13**, 471 (1970).

[3] K. N. Ghia and J. S. Sokhey, Laminar incompressible viscous flow in curved ducts of regular cross-sections, J. Fluids Eng. **99**, 640 (1977).

[4] W. Y. Soh, Developing fluid flow in a curved duct of square cross-section and its fully developed dual solutions, J. Fluid Mech. **188**, 337 (1988).

[5] S. Sugiyama, T. Hayashi, and K. Yamazaki, Flow characteristics in the curved rectangular channels: Visualization of secondary flow, Bull. JSME **26**, 964 (1983).

[6] B. Bara, K. Nandakumar, and J. H. Masliyah, An experimental and numerical study of the Dean problem: Flow development towards two-dimensional multiple solutions, J. Fluid Mech. **244**, 339 (1992).

[7] K. H. Winters, A bifurcation study of laminar flow in a curved tube of rectangular cross-section, J. Fluid Mech. **180**, 343 (1987).

[8] L. Rigo, D. Biau, and X. Gloerfelt, Flow in a weakly curved square duct: Assessment and extension of Dean's model, Phys. Rev. Fluids **6**, 024101 (2021).

[9] P. E. Haines, J. P. Denier, and A. P. Bassom, Dean vortices in finite-aspect-ratio ducts, J. Fluid Mech. **716**, R8 (2013).

[10] N. Nivedita, P. Ligrani, and I. Papautsky, Dean flow dynamics in low-aspect ratio spiral microchannels, Sci. Rep. **7**, 44072 (2017).

[11] V. S. Sivasankar, Y. Wang, R. Natu, D. Porter, L. Herbertson, B. A. Craven, S. Guha, and S. Das, Particle-liquid transport in curved microchannels: Effect of particle volume fraction and size in Dean flow, Phys. Fluids **34**, 053304 (2022).

[12] Q.-V. Do, D.-A. Van, V.-B. Nguyen, and V.-S. Pham, A numerical modeling study on inertial focusing of microparticle in spiral microchannel, AIP Adv. **10**, 075017 (2020).

[13] In their paper, Haines *et al.* [9] defined the Dean number as $(W/R)^{1/2}\rho U_0 W/\mu$ and reported a critical Dean number of about 35 for the transition in secondary flow from one pair of vortices to multiple vortices. We define Dn_W based on the characteristic length $2W$ so that $\mathrm{Dn} = (D_h/2R)^{1/2}\rho U_0 D_h/\mu$ asymptotically approaches Dn_W as $\gamma \to \infty$. This leads to the critical condition $\mathrm{Dn}_W = 2^{3/2}(W/R)^{1/2}\rho U_0 W/\mu \simeq 100$ for the secondary flow transition.

[14] J. T. Ault, K. K. Chen, and H. A. Stone, Downstream decay of fully developed Dean flow, J. Fluid Mech. **777**, 219 (2015).

[15] J. T. Ault, K. K. Chen, and H. A. Stone, Downstream decay of fully developed Dean flow, J. Fluid Mech. **815**, 570 (2017).

[16] S. H. Lee and P. K. Kang, Entry and Exit Flows in Curved Pipes, Phys. Rev. Lett. **124**, 144501 (2020).

[17] D. Vigolo, S. Radi, and H. A. Stone, Unexpected trapping of particles at a T junction, Proc. Natl. Acad. Sci. USA **111**, 4770 (2014).